

Extended Data Table 1 | Dominant ring- and diffuse-porous species at the Smithsonian Conservation Biology Institute (SCBI) and Harvard Forest, along with sample sizes included in this analysis.

	species	dendrometer bands		tree cores	
		n trees	n tree-years	n cores	date range
SCBI					
ring-porous	<i>Carya cordiformis</i>	0	0	18	1917-2009
	<i>Carya glabra</i>	0	0	39	1901-2009
	<i>Carya ovalis</i>	0	0	24	1896-2009
	<i>Carya tomentosa</i>	0	0	17	1926-2009
	<i>Fraxinus nigra</i>	0	0	16	1901-2016
	<i>Fraxinus americana</i>	0	0	69	1910-2009
	<i>Quercus alba</i>	34	272	66	1904-2009
	<i>Quercus montana</i>	0	0	67	1893-2009
	<i>Quercus rubra</i>	33	265	71	1870-2009
	<i>Quercus velutina</i>	0	0	83	1902-2009
diffuse-porous	<i>Fagus grandifolia</i>	13	75	81	1932-2009
	<i>Liriodendron tulipifera</i>	39	292	109	1920-2009
Harvard Forest					
ring-porous	<i>Fraxinus americana</i>	8	28	34	1901-2008
	<i>Quercus rubra</i>	119	529	179	1901-2014
	<i>Quercus velutina</i>	11	53	0	
diffuse-porous	<i>Fagus grandifolia</i>	8	35	0	
	<i>Betula lenta</i>	8	44	0	
	<i>Betula populifolia</i>	5	16	0	
	<i>Betula papyrifera</i>	3	10	0	
	<i>Betula alleghaniensis</i>	19	72	44	1952-2013
	<i>Prunus serotina</i>	8	29	0	
	<i>Acer rubrum</i>	128	477	59	1930-2014
	<i>Acer pensylvanicum</i>	4	13	0	

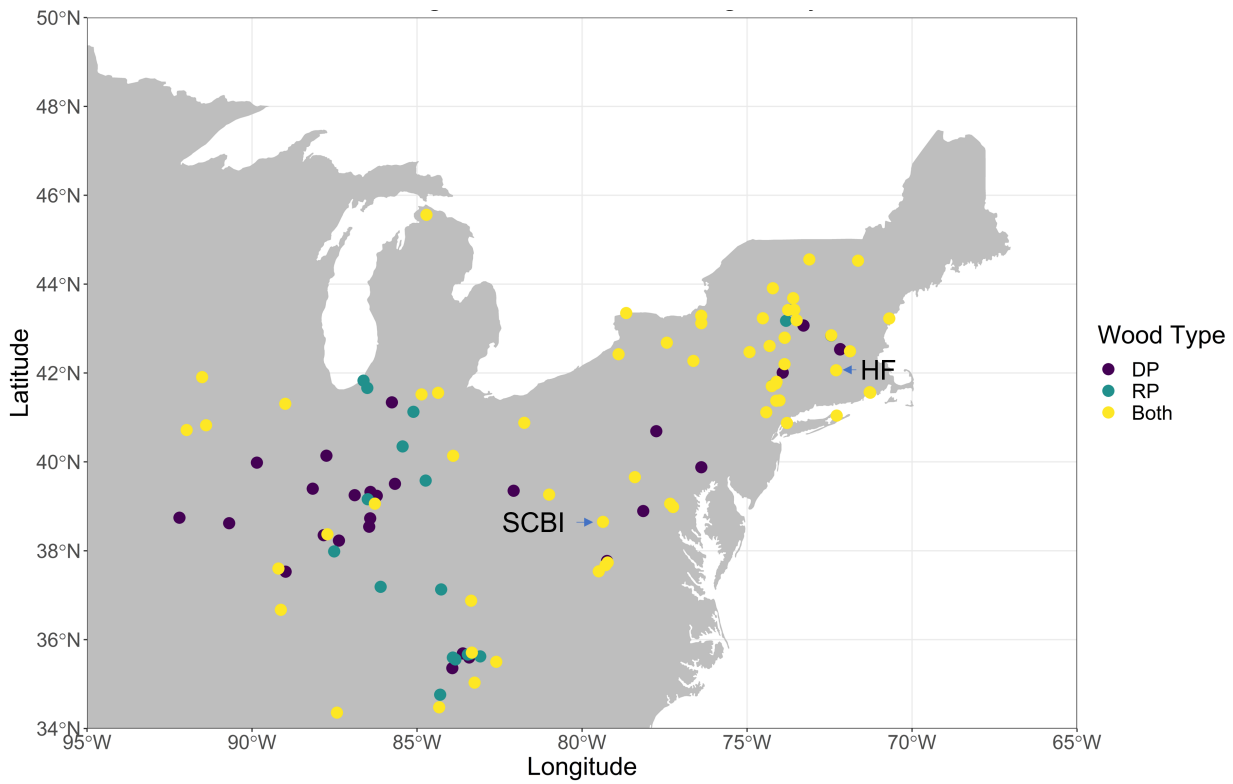
Extended Data Table 2 | Summary of parameters describing the seasonality and temperature sensitivity of ring- and diffuse- porous species groups at the Smithsonian Conservation Biology Institute (SCBI) and Harvard Forest.

	SCBI		Harvard Forest	
	ring-porous	diffuse-porous	ring-porous	diffuse-porous
critical T_{max} window	3/5-3/19	3/19-5/28	3/12-5/21	5/7-6/11
Stem Growth				
DOY_{25}	128 (May 8)	155 (June 5)	144 (May 24)	166 (June 16)
DOY_{50}	154 (June 4)	172 (June 22)	168 (June 17)	183 (July 3)
DOY_{75}	185 (July 4)	190 (July 9)	195 (July 14)	201 (July 20)
g_{max} (cm/day)	0.0043	0.0061	0.003	0.003
L_{pgs}	57.3	34.8	51.3	34.4
ΔDBH (cm/yr)	0.41	0.36	0.26	0.16
Canopy Foliage (ecosystem level)				
Greenup	101 (April 11)		115 (April 25)	
Mid-greenup	121 (May 1)		137 (May 17)	
Peak	173 (June 22)		182 (July 1)	
Senescence	215 (Aug. 3)		218 (Aug. 6)	
Temperature sensitivity* (days/°C)				
Stem growth:				
DOY_{25}	-1.7 ± 0.13	-2.8 ± 0.39	-12.3 ± 0.91	-4.2 ± 0.22
DOY_{50}	-1 ± 0.13	-2.9 ± 0.4	-10.3 ± 0.74	-2.5 ± 0.17
DOY_{75}	0.08 ± 0.19	-2.9 ± 0.6	-11.1 ± 0.96	-0.9 ± 0.23
ΔDBH (cm/°C)	$.003 \pm .001$	$.008 \pm .004$	$-.027 \pm .004$	$-.003 \pm .001$
Canopy foliage:				
Greenup	3.45 ± 1.29		2.4 ± 1.51	
Mid-greenup	3.39 ± 0.86		3.16 ± 0.84	
Peak	4.21 ± 1.70		1.47 ± 1.02	
Senescence	3.85 ± 2.13		0.17 ± 1.53	

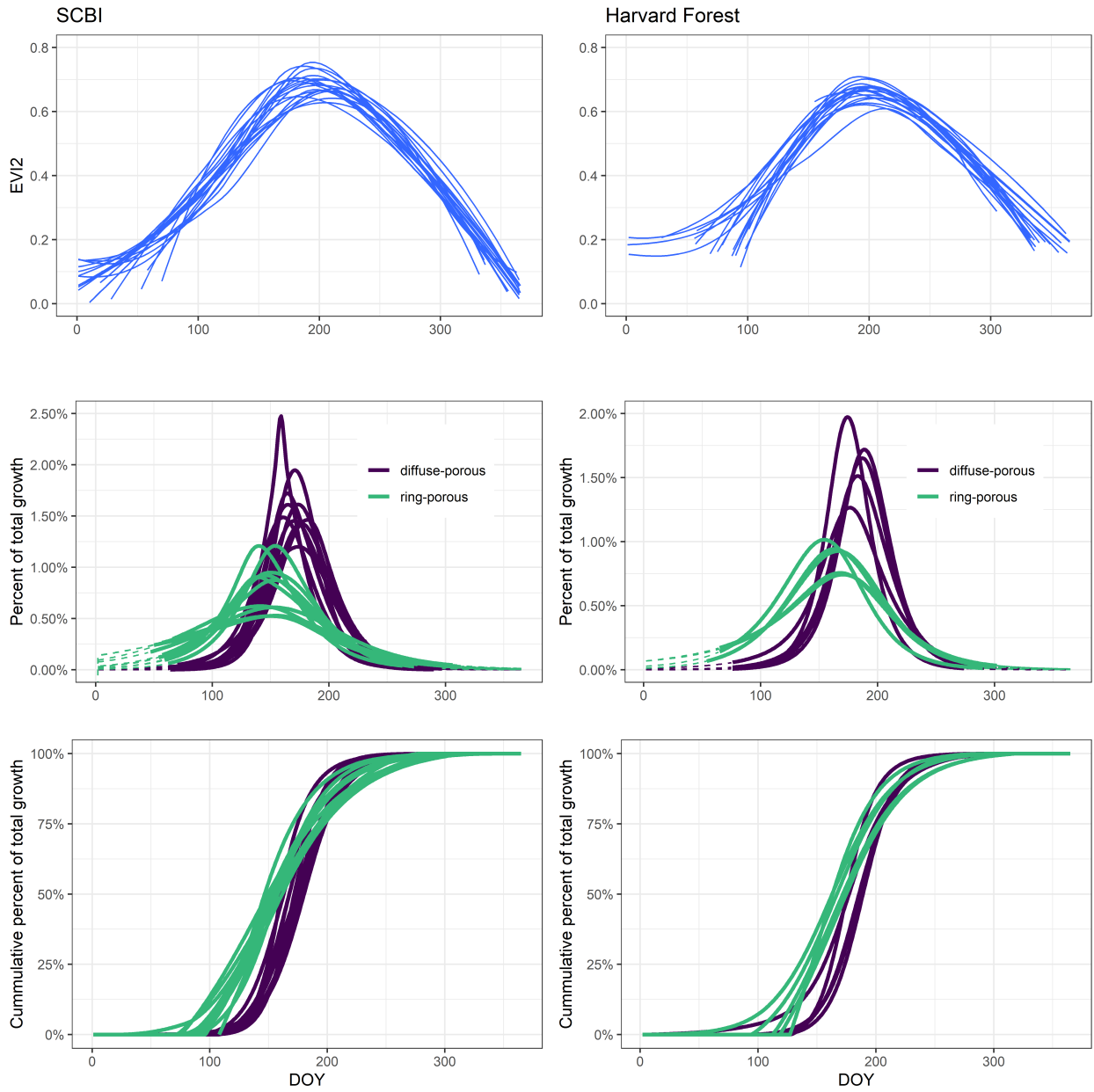
*Temperature sensitivity refers to the sensitivity of a parameter to the mean maximum temperature (T_{max}) during the critical temperature window (CTW, Fig. 1). Because leaf phenology measurements were derived from satellite imagery and included both ring- and diffuse-porous trees, the selection of a critical window was less straightforward. We used the CTW of the porosity group containing the dominant canopy species at each site: *Liriodendron tulipifera* (diffuse porous) at SCBI and *Quercus rubra* (ring porous) at Harvard Forest.

Extended Data Table 3 | Summary of tree-ring chronologies analyzed and number of significant (at $p=0.05$) positive or negative correlations of ring width index to monthly T_{max} in univariate and multivariate analyses.

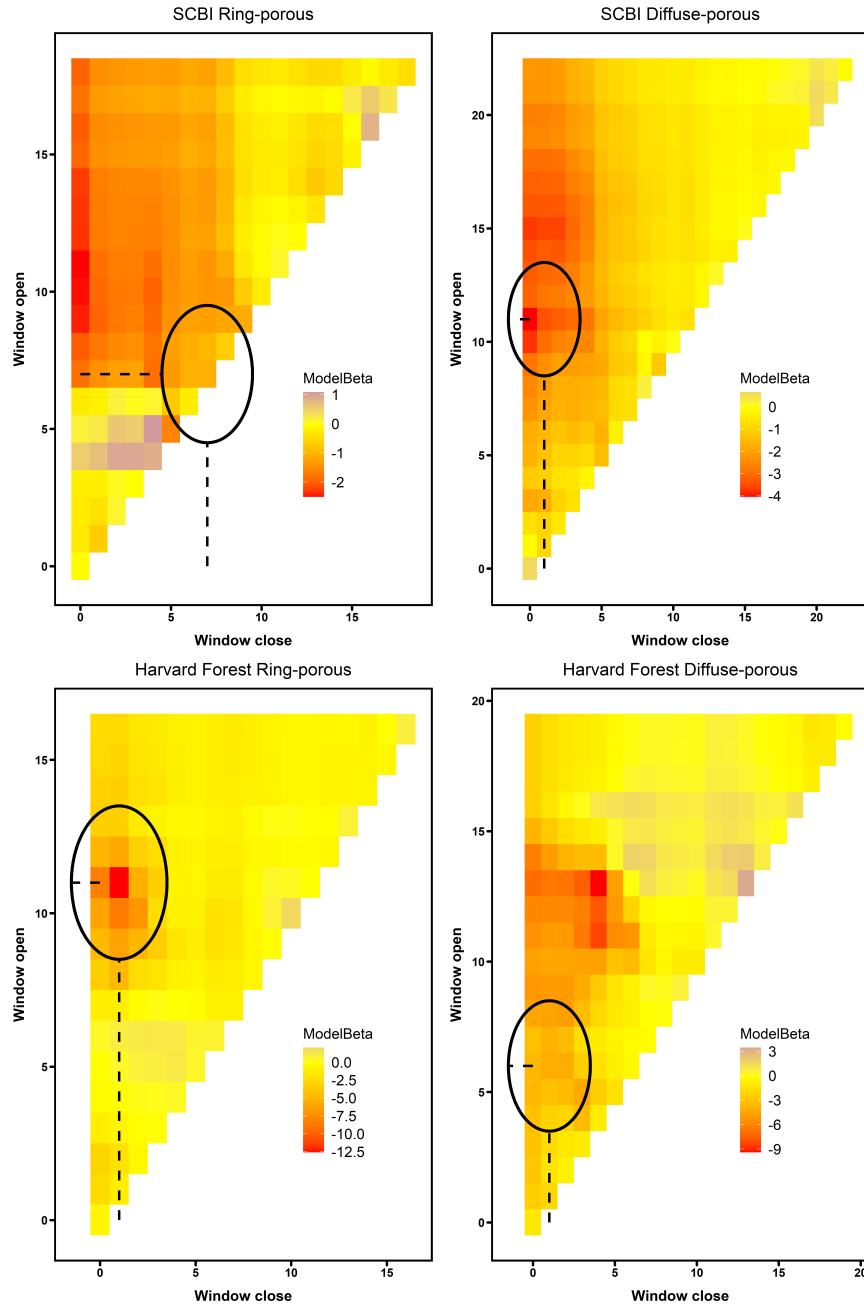
species	n	n. correlations to monthly mean max. T significant at $p=0.05$															
		univariate analysis												multivariate analysis			
		March		April		May		June		July		Aug		April		June-July	
Ring-porous																	
<i>Carya cordiformis</i>	1	0	0	0	0	0	1	0	1	0	0	0	0	0	0	0	1
<i>Carya glabra</i>	7	0	0	0	0	0	3	0	5	0	5	0	0	0	0	0	5
<i>Carya ovalis</i>	1	0	0	1	0	0	1	0	0	0	0	0	1	0	0	0	0
<i>Carya ovata</i>	21	0	2	0	0	0	5	0	20	0	17	0	12	2	0	0	20
<i>Carya tomentosa</i>	2	0	1	0	0	0	1	0	2	0	0	0	2	0	0	0	1
<i>Fraxinus americana</i>	5	0	1	0	0	0	4	0	3	0	2	1	0	0	0	0	3
<i>Fraxinus nigra</i>	2	0	0	0	0	0	0	0	1	0	1	0	1	0	0	0	1
<i>Quercus alba</i>	35	0	2	0	4	0	18	0	31	0	29	0	23	0	2	0	33
<i>Quercus bicolor</i>	1	0	0	0	0	0	0	0	0	0	1	0	1	0	0	0	0
<i>Quercus macrocarpa</i>	1	0	0	0	0	0	0	0	1	0	1	0	1	0	0	0	1
<i>Quercus montana</i>	17	0	1	0	2	1	4	0	10	0	9	0	3	1	2	0	11
<i>Quercus pagoda</i>	1	0	0	0	0	0	1	0	1	0	1	0	1	0	0	0	1
<i>Quercus rubra</i>	37	0	3	0	2	1	4	0	25	0	18	1	5	1	1	0	22
<i>Quercus sp</i> (white oak group)	1	0	0	0	0	0	0	0	1	0	0	0	0	0	0	0	1
<i>Quercus stellata</i>	2	0	0	0	0	0	1	0	1	0	1	0	0	0	0	0	1
<i>Quercus velutina</i>	7	0	0	0	0	0	2	0	5	0	6	0	3	0	0	0	7
TOTAL	141	0	10	1	8	2	45	0	107	0	91	2	53	4	5	0	108
Diffuse-porous																	
<i>Acer rubrum</i>	4	0	0	0	1	0	0	0	1	0	1	0	0	0	1	0	3
<i>Acer saccharum</i>	16	0	0	1	0	0	2	0	14	0	12	0	6	3	0	0	14
<i>Betula alleghaniensis</i>	2	0	0	0	0	0	0	0	2	0	0	0	0	0	0	0	1
<i>Betula lenta</i>	3	0	0	0	0	0	1	0	1	0	1	0	0	0	0	0	2
<i>Fagus grandifolia</i>	6	0	0	1	0	0	0	0	4	0	5	0	1	1	0	0	5
<i>Liriodendron tulipifera</i>	32	0	0	2	1	0	7	0	30	0	17	0	16	1	0	0	27
<i>Magnolia acuminata</i>	1	0	0	0	0	0	0	0	0	0	0	0	0	0	0	0	0
<i>Nyssa sylvatica</i>	1	0	0	0	0	0	0	0	0	0	0	0	0	0	0	0	0
<i>Populus grandidentata</i>	1	0	0	0	0	0	0	0	0	0	0	0	0	0	0	0	0
TOTAL	66	0	0	4	2	0	10	0	52	0	36	0	23	5	1	0	52
TOTAL	207	0	10	5	10	2	55	0	159	0	127	2	76	9	6	0	160



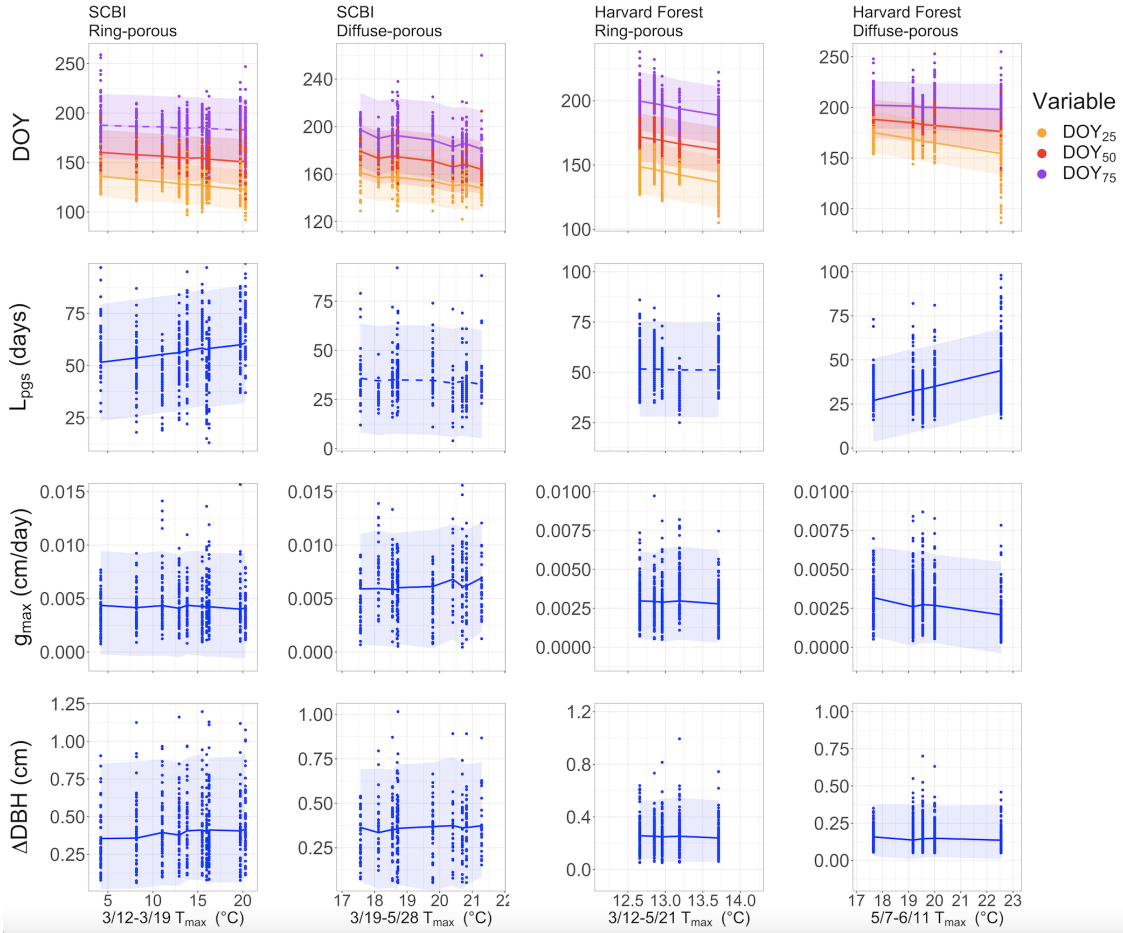
Extended Data Figure 1 | Map of sampling locations of tree-ring chronologies analyzed in this study. Sites are colored by the xylem porosity type of species sampled: ring porous (RP), diffuse porous (DP), or both. Sampling details are provided in SI Table 1.



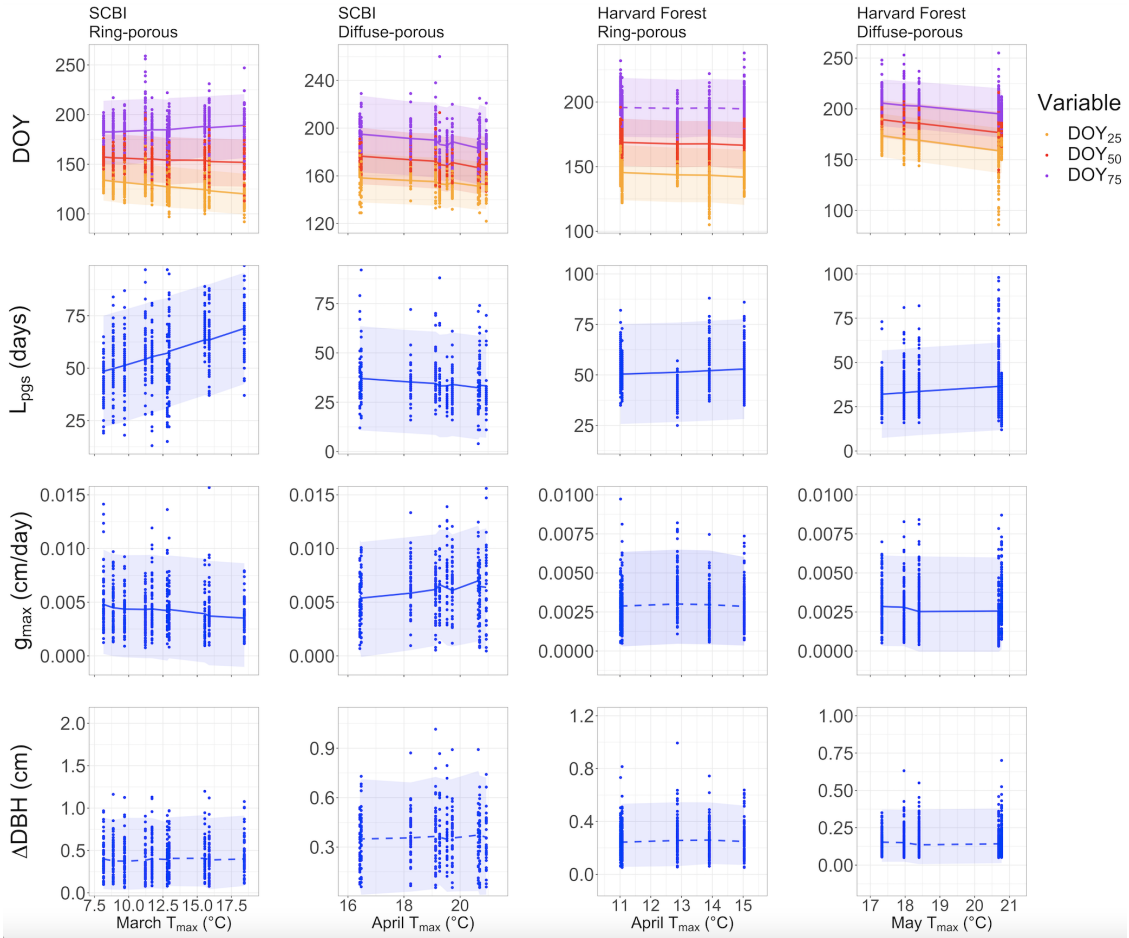
Extended Data Figure 2 | Phenological patterns of forest canopy greenness (top row) and stem growth of ring- and diffuse-porous trees, represented as both relative and cumulative fractions of total annual growth (middle and bottom rows, respectively), at the Smithsonian Conservation Biology Institute (SCBI) and Harvard Forest. In the top row, canopy greenness is characterized using the two band Enhanced Vegetation Index (EVI2), with each line representing a year between 2000 and 2018. For stem growth, each line represents the average growth over one year, as modeled based on a five-parameter logistic growth model to dendrometer band data. Dashed lines represent modeled DBH change which fell outside of the median DOY where predicted starting DBH (a) and predicted ending DBH (b) were reached. Solid lines represent DBH change attributable to stem growth.



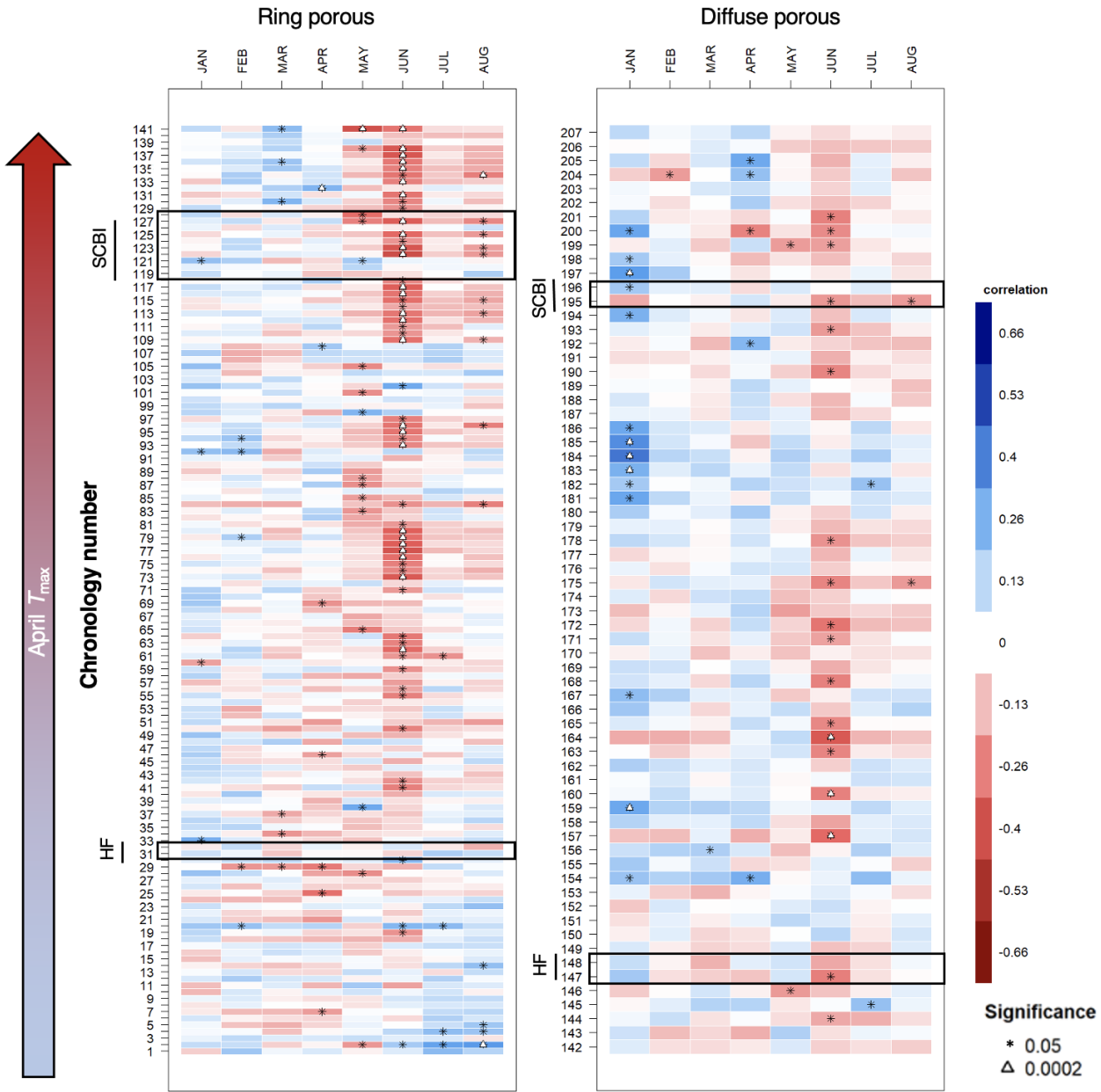
Extended Data Figure 3 | Landscapes of relationships between the day of year on which 25% of annual growth is achieved (DOY_{25}) and temperature in prior weeks for ring- and diffuse-porous trees at the Smithsonian Conservation Biology Institute (SCBI) and Harvard Forest. Shown are matrices of β coefficients from first-order linear regressions between mean maximum temperature (T_{max}) and DOY_{25} . Window Open and Window Close indicate number of weeks prior to DOY_{25} (listed in Extended Data Table 2). Yellow shading indicates neutral relationships, while orange or red shading indicates that DOY_{25} advances with increased T_{max} over the given time window (negative β). Black circles indicate the critical temperature window selected based on minimization of $\Delta AICc$, the difference in Akaike Information Criterion corrected for small sample size relative to a null model. Critical temperature windows are listed in Extended Data Table 2.



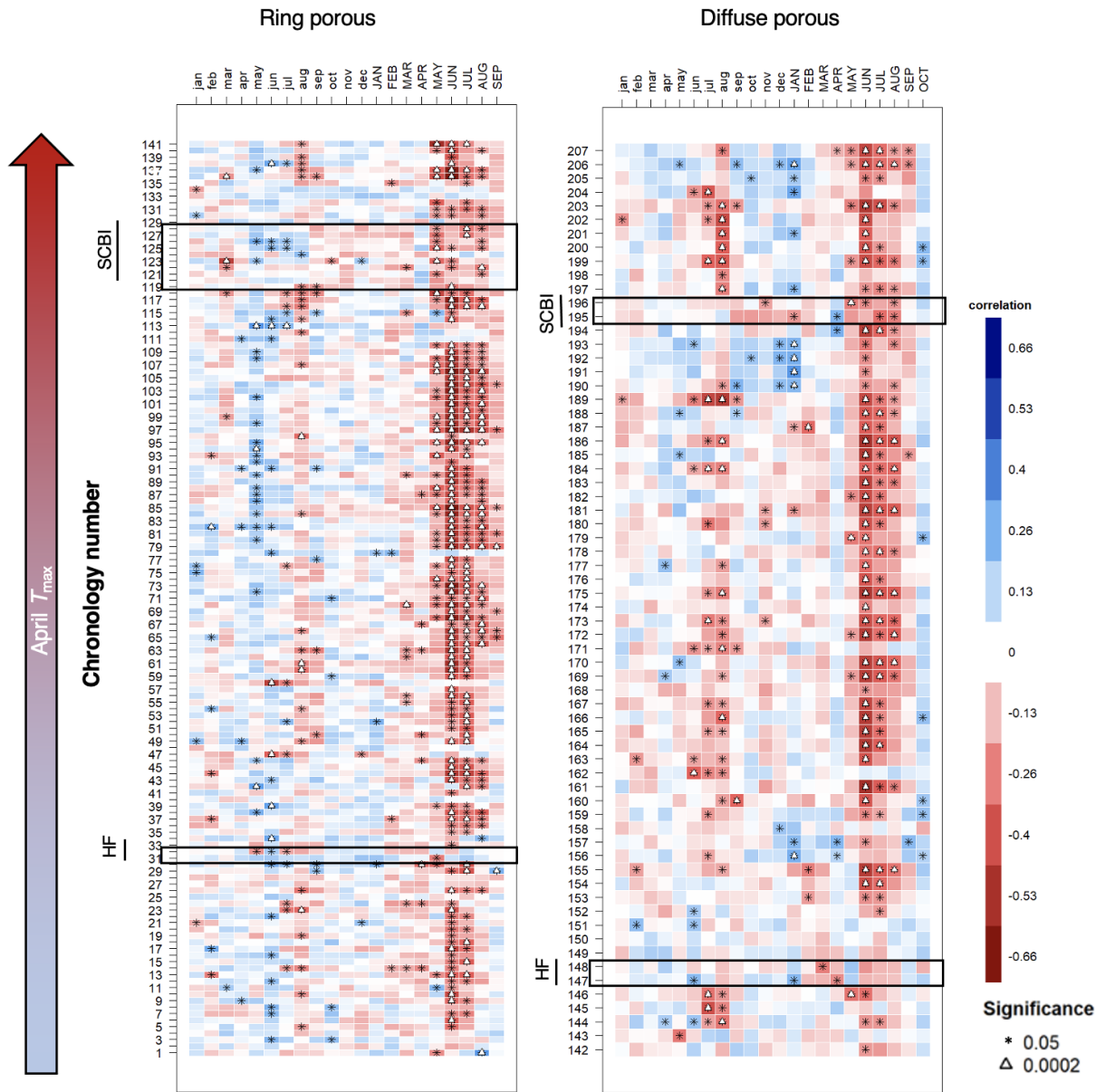
Extended Data Figure 4 | Response of stem growth timing and rates to mean maximum temperatures (T_{max}) during the spring critical temperature window (CTW) for ring- and diffuse-porous species at the Smithsonian Conservation Biology Institute (SCBI) and Harvard Forest. CTW was defined as the period over which T_{max} was most strongly correlated with the day of year on which 25% of annual growth was achieved (DOY_{25} ; Extended Data Table 2, Extended Data Figure 3). Shown are relationships between mean T_{max} over the CTW and days of the year on which 25%, 50%, and 75% total stem growth were achieved (DOY_{25} , DOY_{50} , DOY_{75} , respectively; first row); the length of the peak growing season (L_{pgs} ; second row); maximum growth rate (g_{max} ; third row); and total seasonal radial stem growth (ΔDBH ; fourth row). Posterior predictions of each variable that did not include zero are represented with solid lines, while those that do include zero use dotted lines. 95% credible intervals are represented by bands. For both species groups at both sites, DOY_{25} , DOY_{50} , and DOY_{75} all declined significantly with mean T_{max} during their respective CTW. Dots represent growth parameter values for individual tree-year combinations, which were derived by fitting a five-parameter logistic growth model to dendrometer band data.



Extended Data Figure 5 | Response of stem growth timing and rates to mean maximum temperatures (T_{max}) for the month most closely corresponding to the spring critical temperature window (CTW) for ring- and diffuse-porous species at the Smithsonian Conservation Biology Institute (SCBI) and Harvard Forest. CTW was defined as the period over which T_{max} was most strongly correlated with the day of year on which 25% of annual growth was achieved (DOY_{25} ; Extended Data Table 2, Extended Data Figure 3), and the most closely corresponding month was determined as that with the greatest number of days within the CTW. Shown are relationships between monthly T_{max} and days of the year on which 25%, 50%, and 75% total stem growth were achieved (DOY_{25} , DOY_{50} , DOY_{75} , respectively; first row); the length of the peak growing season (L_{pgs} ; second row); maximum growth rate (g_{max} ; third row); and total seasonal radial stem growth (ΔDBH ; fourth row). Posterior predictions of each variable that did not include zero are represented with solid lines, while those that do include zero use dotted lines. 95% credible intervals are represented by bands. For both species groups at both sites, DOY_{25} , DOY_{50} , and DOY_{75} declined significantly with April T_{max} , with the exception of DOY_{25} for ring-porous species at SCBI. Dots represent growth parameter values for individual tree-year combinations, which were derived by fitting a five-parameter logistic growth model to dendrometer band data.



Extended Data Figure 6 | Sensitivity of annual growth, as derived from tree-rings, to monthly mean minimum temperatures (T_{min}), for 207 chronologies from 108 sites across eastern North America (Extended Data Figure 1). Colors indicate the correlation between monthly T_{min} and a dimensionless ring width index (RWI) derived from the multiple trees that form each chronology and emphasizing interannual variability associated with climate. Chronologies are grouped by xylem porosity and ordered by mean April T_{min} . Plots are annotated to highlight records from our two focal sites, the Smithsonian Conservation Biology Institute (SCBI) and Harvard Forest (HF) (Extended Data Table 1). Species analyzed and numbers of significant correlations to T_{min} are summarized in Extended Data Table 3, and chronology details are given in SI Table 1.



Extended Data Figure 7 | Sensitivity of annual growth, as derived from tree-rings, to monthly mean maximum temperatures (T_{max}) of the current and past year, for 207 chronologies from 108 sites across eastern North America (Extended Data Figure 1). Colors indicate the correlation between monthly T_{max} and a dimensionless ring width index (RWI) derived from the multiple trees that form each chronology and emphasizing interannual variability associated with climate. Chronologies are grouped by xylem porosity and ordered by mean April T_{max} . Plots are annotated to highlight records from our two focal sites, the Smithsonian Conservation Biology Institute (SCBI) and Harvard Forest (HF) (Extended Data Table 1). Figure presents the same results as main manuscript Fig. 3 but extends back to include the previous year. Species analyzed and numbers of significant correlations to T_{max} are summarized in Extended Data Table 3, and chronology details are given in SI Table 1.